



HAL
open science

Mistuning Identification and Model Updating of an Industrial Blisk

D. Laxalde, Fabrice Thouverez, Jean-Jacques Sinou, J.-P. Lombard, S. Baumhauer

► **To cite this version:**

D. Laxalde, Fabrice Thouverez, Jean-Jacques Sinou, J.-P. Lombard, S. Baumhauer. Mistuning Identification and Model Updating of an Industrial Blisk. *International Journal of Rotating Machinery*, 2007, 2007 (Article ID 17289), pp.1-10. 10.1155/2007/17289 . hal-00214219

HAL Id: hal-00214219

<https://hal.science/hal-00214219v1>

Submitted on 23 Jan 2008

HAL is a multi-disciplinary open access archive for the deposit and dissemination of scientific research documents, whether they are published or not. The documents may come from teaching and research institutions in France or abroad, or from public or private research centers.

L'archive ouverte pluridisciplinaire **HAL**, est destinée au dépôt et à la diffusion de documents scientifiques de niveau recherche, publiés ou non, émanant des établissements d'enseignement et de recherche français ou étrangers, des laboratoires publics ou privés.

Review Article

Mistuning Identification and Model Updating of an Industrial Blisk

D. Laxalde,^{1,2} F. Thouverez,¹ J.-J. Sinou,¹ J.-P. Lombard,² and S. Baumhauer²

¹Laboratoire de Tribologie et Dynamique des Systèmes, Équipe Dynamique des Structures et des Systèmes, École Centrale de Lyon, 36 avenue Guy de Collongue, 69134 Ecully Cedex, France

²Snecma (Safran group), 77550 Moissy-Cramayel, France

Received 16 February 2006; Revised 6 December 2006; Accepted 6 December 2006

Recommended by Agnes Muszynska

The results of a complete study of mistuning identification on an industrial blisk are presented. The identification method used here is based on a model-updating technique of a reduced order. This reduced-order model is built using component mode synthesis, and mistuning is introduced as perturbations of the cantilevered-blade modes. The measured modal data are extracted from global measurements of the blisk's forced response. As we use a single point excitation, this measurement procedure allows the acquisition of all the modes of a given family with a quite simple experimental set-up. A selection of the best identified modal data is finally performed. During the mistuning identification procedure, these measured data are regularized using an eigenvector assignment technique which reduces the influence of eventual measurement errors. An inverse problem, based on the perturbed (mistuned) modal equation, is defined with measured modes as input and mistuning parameters as unknown. Then, the reduced-order model is updated with the identified mistuning, we first perform a correlation on modal responses (using eigenfrequency deviation criteria and MACs). Finally, correlation results on forced responses are presented and discussed.

Copyright © 2007 D. Laxalde et al. This is an open access article distributed under the Creative Commons Attribution License, which permits unrestricted use, distribution, and reproduction in any medium, provided the original work is properly cited.

1. INTRODUCTION

Mistuning of turbomachinery bladed disks refers to small variations of structural or geometrical properties between each sector. These variations may result from various causes such as manufacturing process, material inhomogeneity or eventually wear and are then inevitable [1]. The dynamics of mistuned bladed disks can significantly differ from the tuned case [2, 3]. In free response, mistuning results in a nonuniform distribution (localization) of the vibratory energy around the structure. In forced response, resonant amplitudes of some blades are significantly increased due to this localization phenomenon and this can lead to high-cycle fatigue, wear or rupture in the worst cases.

From these considerations, mistuning needs to be considered in the design of bladed disk and several ways of investigations can be highlighted. First, representative models of mistuned bladed disks need to be developed; however, since the structure is no longer assumed to be cyclically symmetric, this assumption cannot be used in the finite element modeling to reduce the size of the problem. Since the full (360°) FE modeling and calculations cannot be applied for obvious

reasons, component mode synthesis methods are now commonly used. An overview of existent methods can be found for example in [4–8], where it can be seen that the computational costs are highly reduced when using reduced-order models as compared to FE analysis and with some good accuracy. In this paper, a classical component-mode synthesis method adapted to cyclic structures will be used in order to build a representative model of mistuned bladed disk.

Another issue concerning the study of mistuned bladed disks is the ability to predict the resonant response to random mistuning distribution. This is usually done through statistical approaches [9, 10] where the use of ROMs become imperative as well as some good knowledge of the mistuning data (statistic or possibilistic). This last point is the subject of this article. In effect, mistuning can only be known through an experimental approach.

In bladed disk assemblies, measurements on the individual blades lead to both their natural frequencies and structural properties; then, in a first approximation, the mistuning of the assembled bladed disk can be known. However, concerning one-piece structures such as blisks (integrally bladed disks), since blades cannot be removed for individual

measurements and mistuning identification can only be achieved through global measurements on the whole structure followed by a global model updating procedure. Mistuning of bladed disks was studied experimentally by Judge et al. [11] who verify the localization effects and amplification of the forced response. In recent years, several methods of mistuning identification were developed. Judge et al. [12] have proposed an identification technique which uses measurements of a system of modes and gives the mistuning parameters of the reduced-order model proposed by Bladh et al. [7]. Feiner and Griffin [13, 14] have proposed a method of identification for a whole sector of a bladed disk based on a reduced-order modelling method called fundamental mistuning model, they also proposed a completely experimental strategy. Another method, proposed by Pichot et al. [15] and used in this study, is also based on a component mode synthesis and uses an original technique of eigenvalue assignment [16, 17] combined with a regularization technique which minimizes the effect of measurement errors. This method was numerically validated in [18].

This paper presents the results of a complete investigation of mistuning identification on an industrial blisk in which the mistuning is not a priori known. In the first part, we will briefly present the mistuning identification technique used as well as an associated modelling method of mistuning bladed disks. The complete experimental investigations, adapted to industrial blisks in regard to its simplicity procedure, are presented followed by the identification and model updating procedures; then, the correlation results on modal and forced responses are presented.

2. MODEL OF MISTUNED BLADED DISKS

2.1. Cyclic symmetry reduction

The dynamic behaviour of cyclic structures (or rotationally periodic structures) can be analysed by considering only one reference sector and applying appropriate boundary conditions with the adjacent sectors, without any approximation. Considering a structure with N sectors, the displacements of any sector n can be related to the displacements of the reference sector 1 by the phase angle $\alpha = 2\pi/N$ as

$$\mathbf{u}^{(n)} = \Re \sum_{p=0}^{N-1} e^{i(n-1)p\alpha} \bar{\mathbf{u}}_p^{(1)}, \quad (1)$$

where $\bar{\mathbf{u}}_p^{(1)}$ is the displacements vector of the reference sector expressed in travelling wave coordinates for the phase number p (nodal diameter).

2.2. Component-mode synthesis

The use of reduced-order modelling techniques is now common to study the impact of mistuning in turbomachinery bladed disks. In early developments, these took the form of lumped-parameter modelling and now component-mode synthesis methods are widely used. Various reduced-order models have been proposed in the literature [4, 7, 19] and,

recently, some more efficient methods have been developed which require fewer input data [5].

The method used in this study is similar to the component mode substitution method of Benfield and Hruda [20], and is adapted to bladed disk modelling. The main advantage is that mistuning can be easily introduced as a perturbation of the cantilevered-blade modes.

Theory

Considering a bladed-disk elementary sector, we define two substructures which are the disk and the blade (and the associated interface). The motion of the entire bladed disk is described using two sets of modes: disk modes with loaded interface (all nodal diameters) and cantilevered-blade modes; both of these modal families being extracted from a finite-element analysis.

The blade component modes are derived using a Craig-Bampton technique [21], with

- (i) Φ_b , a truncated series of normal modes of vibration with fixed interface as boundary conditions;
- (ii) Ψ , a set of constraint modes which are the static deformation shapes of the blade component obtained by imposing successively a unit displacement on one interface coordinate, while holding the remaining interface coordinate fixed.

The physical displacement vector of a single blade is

$$\bar{\mathbf{u}}_b = \bar{\Phi}_b \mathbf{q}_b + \bar{\Psi} \mathbf{u}_j. \quad (2)$$

Then, using the cyclic extension procedure derived in Section 2.1, we can express the displacement of all blades so that

$$\mathbf{u}_b = \Phi_b \mathbf{q}_b + \Psi \mathbf{u}_j. \quad (3)$$

The displacement of the disk component is represented by a truncation of normal modes with loaded interface expressed in travelling wave coordinates (for all possible nodal diameters):

$$\mathbf{u}_d = \sum_{p=0}^{N-1} \Phi_d^p \mathbf{q}_d^p = \Phi_d \mathbf{q}_d. \quad (4)$$

Then, considering the displacement compatibility at the interface, one finds

$$\mathbf{u}_b = \Phi_b \mathbf{q}_b + \Psi \Phi_{d,j} \mathbf{q}_d, \quad (5)$$

where $\Phi_{d,j}$ is the restriction of the disk modes in travelling coordinates Φ_d to the interface degrees of freedom.

Assembling the substructures, the bladed disk's displacements are expressed as a function of the modal coordinates \mathbf{q} only (with no physical displacements of the interface remaining) and the transformation from physical coordinates to generalized coordinates is done using the transformation matrix T defined as

$$\begin{bmatrix} \mathbf{u}_b \\ \mathbf{u}_d \end{bmatrix} = T \begin{bmatrix} \mathbf{q}_b \\ \mathbf{q}_d \end{bmatrix} \quad \text{with } T = \begin{bmatrix} \Phi_b & \Psi \Phi_{d,j} \\ 0 & \Phi_d \end{bmatrix}. \quad (6)$$

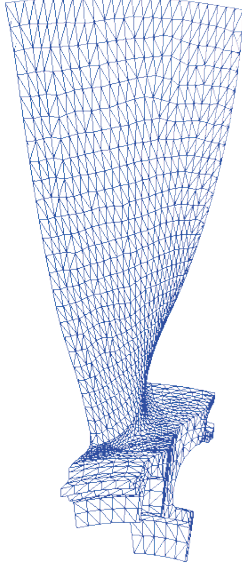


FIGURE 1: FE model of the blisk.

Finally, the modal matrices are expressed:

$$\bar{K} = T^T \begin{bmatrix} K_b & 0 \\ 0 & K_d \end{bmatrix} T = \begin{bmatrix} \bar{K}_{bb} & \bar{K}_{bd} \\ \bar{K}_{db} & \bar{K}_{dd} \end{bmatrix}, \quad (7a)$$

$$\bar{M} = T^T \begin{bmatrix} M_b & 0 \\ 0 & M_d \end{bmatrix} T = \begin{bmatrix} \bar{M}_{bb} & \bar{M}_{bd} \\ \bar{M}_{db} & \bar{M}_{dd} \end{bmatrix}, \quad (7b)$$

where the superscript T denotes the transposition.

Application on a blisk

In this study, we focus on the blisk whose finite-element model is depicted in Figure 1 (elementary sector). This piece is a low-pressure compressor stage blisk provided by Snecma and has 24 blades with a rather complex geometry. This FE model has around 180 000 degrees-of-freedom in each sector. The natural frequencies of this blisk are plotted against the nodal diameter in Figure 2. The eigenfrequency/nodal diameter representation is typical of bladed disks analysis. In effect, as briefly described in Section 2.1, the modes of cyclic structures have modes of nodal diameter type which can be, using the (exact) cyclic symmetry reduction, studied separately. Each nodal diameter family is independent from each other which justifies the frequency/nodal diameter plot of Figure 2.

A reduced-order model of this blisk is then constructed using the technique presented in the previous section; the input data of this model (i.e., the modes) were chosen so that it correctly represents the behaviour of the first two modal families of the blisk which are the first bending modes of the blades. This reduced-order model has now 400 dof, which are 10 cantilevered-blade modes and from 5 to 2 disk modes in each nodal diameter.

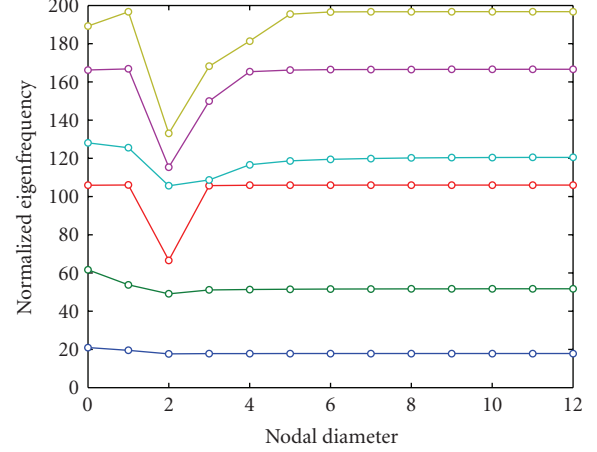


FIGURE 2: Frequency/nodal diameter diagram.

2.3. Mistuning representation

Of interest is to build a model of mistuned bladed disk that accurately predicts modal or forced responses of a mistuned structures. The issue is then how to model the variations of structural properties (mistuning) to achieve this goal. As pointed out by Mignolet et al. [22] among others, assuming small perturbations, an accurate knowledge of all structural parameters is not always necessary to get good predictions of global responses. Rather, the identification of modal characteristics can be sufficient. Several types of mistuning have been defined in the literature, depending on which modal properties are affected by mistuning. These are the frequency, the damping, and the shape mistunings, each of these referring to changes in the natural frequencies, damping ratio, or deformed shapes induced by structural mistuning. Generally, only frequency mistuning of the blades is considered, assuming the disk to be symmetric. Then, mistuning is introduced as perturbations p_i of the Young's modulus of individual blades. It is introduced *a posteriori* in the reduced stiffness matrix in the blades elements (7a). The perturbed stiffness matrix of the blades is then given by

$$\bar{K}_{bb} = \text{diag}(1 + p_i) \otimes K_{bb}. \quad (8)$$

3. MISTUNING IDENTIFICATION TECHNIQUE

The mistuning identification technique used for this study was presented by Pichot et al. [15, 18, 23]. This method aims at updating the previous mistuned reduced-order model of bladed disk. An inverse problem is defined using the equations of the reduced-order model and, given a set of measured (mistuned) modes and natural frequencies, the proper mistuning parameters (\mathbf{p} vector) can be found. This inverse problem is then solved using a direct least-square procedure.

This type of approach is quite usual in model-updating techniques and was used in previously mentioned works on mistuning identification; Judge's method is also based on a component mode synthesis ROM whereas Feiner's method

is based on a non-CMS fundamental mistuning model. The main feature of Pichot's method is the use of a particular regularization method for the measured data. This method uses the eigenvalue assignment technique proposed by Lim [16, 17]. This identification method and its implementation were validated numerically in Pichot's works and will be briefly reviewed in this part.

3.1. Inverse problem definition

The identification is done using the mistuned eigenvalue equation expressed in modal coordinates (superscripts r), which is

$$K_M \Phi^r = M \Phi^r \Lambda^r, \quad (9)$$

where Φ^r and Λ^r are matrices containing reduced eigenvectors and eigenvalues (extracted from measured FRFs), and K_M is the mistuned stiffness matrix expressed using (8) for the whole structure as

$$K_M = K_T + \sum_{i=1}^N p_i {}^i K \quad (10)$$

and ${}^i K$ is the stiffness matrix of the i th blade.

Combining (9) and (10) leads to

$$\sum_{i=1}^N p_i {}^i K \Phi^r = M \Phi^r \Lambda^r - K_T \Phi^r, \quad (11)$$

which is the basic equation of the inverse problem. The mistuned eigenvectors φ_j^r and associated natural frequencies ω_j are known inputs of the problem, and the mistuning parameters p_i are the unknowns. Next, this base-equation (11) will first be used in a filtering procedure of the measured modes and then to identify the mistuned parameters.

3.2. Expansion-reduction steps for measured data

The experimental data often provide fewer information than the model (reduced-order) to be updated; for example, not all the modes of the family of interest can be identified. As a consequence, an expansion of these measured data is required before we should compare them with FE model's data to be updated. Since this expansion procedure can be computationally expensive when dealing with large FE models, we perform this expansion step on a restricted number of nodes and degrees of freedom. We choose a subset of nodes in the FE model so that it properly represents the deformed shape of the mode we study. The number of nodes required depends on the target mode; usually, about a hundred nodes provide a rather good representation of the global deformed shape. As an example, the retained node for the first bending mode as represented by red lozenges in Figure 3. The expansion method used is a modal expansion:

- (i) we search the expanded eigenvector φ as a linear combination of analytical (tuned) eigenvectors Φ :

$$\varphi = \begin{bmatrix} \varphi_m \\ \varphi_e \end{bmatrix} = \Phi \mathbf{q} = \begin{bmatrix} \Phi_m \\ \Phi_e \end{bmatrix} \mathbf{q}, \quad (12)$$

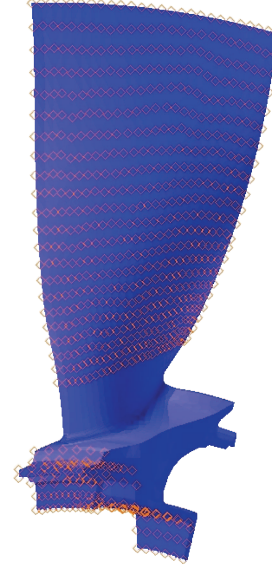


FIGURE 3: Retained nodes \diamond for the 1st mode.

where the subscripts m and e refer to measured dofs and other dofs, respectively,

- (ii) the vector \mathbf{q} is calculated to minimize the error between the measured eigenvector φ_x and modal projection φ_m using a least square minimization:

$$\mathbf{q} = \Phi_m^+ \varphi_x, \quad (13)$$

where the superscript $+$ refers to the Moore-Penrose pseudoinverse.

To sum up, starting from the measured modes φ_x , \mathbf{q} is calculated through (13) and then (12) is used to obtain the expanded modes.

The main equation (11) of the mistuning identification problem is expressed in generalized coordinates, so the measured eigenvectors previously expanded need to be transformed in modal coordinates using (6):

$$\varphi^r = T \varphi. \quad (14)$$

3.3. Eigenvalue assignment and regularization techniques

As mentioned earlier, the first step of the identification procedure is filtering of the measured data in order to increase their representativeness. This is done through an eigendata assignment technique of all measured modes simultaneously. The latter, presented by Lim et al. [16, 17], is called the *best achievable eigenvectors* and consists in a projection of the measured eigenvectors on a subspace spanned by the perturbed model. It is combined with a regularization of measured eigenvectors in order to eliminate part of measured modes which are not realizable with mistuned model considered. Both methods are presented in this part.

Concerning the eigenvalue assignment, we start from (11) expressed for each j eigenvectors φ_j^r separately, and

assuming the mistuned natural frequencies to be distinct from the tuned ones, we find

$$\sum_{i=1}^N p_i E_j^{-1} {}^i K \boldsymbol{\varphi}_j^r = \boldsymbol{\varphi}_j^r, \quad (15)$$

where

$$E_j = (\omega_j^2 M - K_T). \quad (16)$$

With (15), one can notice that each eigenvector can be interpreted as a sum of vectors weighted by the mistuning parameters. As a consequence, (15) is rewritten in the following matrix form:

$$L_j \boldsymbol{\gamma}_j = \boldsymbol{\varphi}_j^r, \quad (17)$$

where

$$L_j = [E_j^{-1} \cdot {}^1 K \quad E_j^{-1} \cdot {}^2 K \quad \cdots \quad E_j^{-1} \cdot {}^N K], \quad (18)$$

$$\boldsymbol{\gamma}_j = [p_1 \boldsymbol{\varphi}_j^r p_2 \boldsymbol{\varphi}_j^r \quad \cdots \quad p_N \boldsymbol{\varphi}_j^r]^T. \quad (19)$$

With (17), one can now notice that $\boldsymbol{\varphi}_j^r$ must lie in the subspace spanned by the columns of L_j , which are only dependent of the tuned system matrices and of the eigenfrequency ω_j whereas both the mistuning parameters p_i and j th eigenvector $\boldsymbol{\varphi}_j^r$ are included in the vector $\boldsymbol{\gamma}_j$. Equation (17) is however not verified in practice because of measurements noise or nonlinearities not taken into account in the model. As a consequence, a regularization step is required to achieve this condition.

Regularization consists in the projection of each measured eigenvector $\boldsymbol{\varphi}_j^r$ on the subspace of the possible solutions for the analytical mistuned system. For this, an optimal vector $\boldsymbol{\gamma}_j$ is calculated to satisfy (17):

$$\boldsymbol{\gamma}_j = L_j^+ \boldsymbol{\varphi}_j^r, \quad (20)$$

where the superscript $+$ refers to the Moore-Penrose pseudoinverse, used when performing a least square minimization.

Then combining (18) and (20), we find the final expression of the regularized eigenvector:

$$\boldsymbol{\varphi}_j^{rf} = L_j L_j^+ \boldsymbol{\varphi}_j^r. \quad (21)$$

This equation defines the best achievable eigenvector, that is, an eigenvector which is realizable with mistuning parameters values p_i .

Then the resolution is realized with the modal matrix of filtered eigenvectors using (11):

$$\sum_{i=1}^N p_i {}^i K \Phi^{rf} = M \Phi^{rf} \Lambda^r - K_T \Phi^{rf}. \quad (22)$$

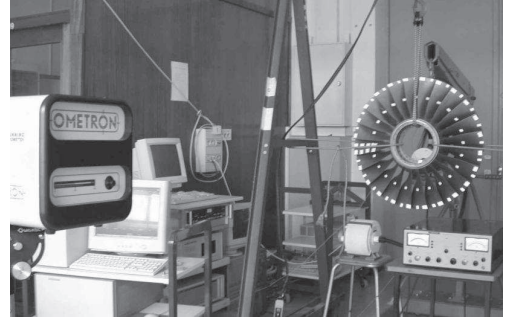


FIGURE 4: Global experimental set-up.

3.4. Identification of mistuning parameters

To solve the final mistuning problem defined by (22), a least square fit strategy is used (which is quite usual in model updating techniques and was also used in other mistuning identification techniques [13]). The aim is to determine parameters p_i , so they are isolated in a vector \boldsymbol{p} :

$$\hat{L} \boldsymbol{p} = R, \quad (23)$$

where

$$\hat{L} = \begin{bmatrix} {}^1 K \boldsymbol{\varphi}_1^{rf} & {}^2 K \boldsymbol{\varphi}_1^{rf} & \cdots & {}^N K \boldsymbol{\varphi}_1^{rf} \\ {}^1 K \boldsymbol{\varphi}_2^{rf} & {}^2 K \boldsymbol{\varphi}_2^{rf} & \cdots & {}^N K \boldsymbol{\varphi}_2^{rf} \\ \vdots & \vdots & \ddots & \vdots \\ {}^1 K \boldsymbol{\varphi}_r^{rf} & {}^2 K \boldsymbol{\varphi}_r^{rf} & \cdots & {}^N K \boldsymbol{\varphi}_r^{rf} \end{bmatrix}, \quad (24)$$

$$R = \begin{bmatrix} M \boldsymbol{\varphi}_1^{rf} \omega_1^2 - K_T \boldsymbol{\varphi}_1^{rf} \\ M \boldsymbol{\varphi}_2^{rf} \omega_2^2 - K_T \boldsymbol{\varphi}_2^{rf} \\ \vdots \\ M \boldsymbol{\varphi}_r^{rf} \omega_r^2 - K_T \boldsymbol{\varphi}_r^{rf} \end{bmatrix}.$$

This vector \boldsymbol{p} is then estimated using a least square procedure:

$$\boldsymbol{p} = \hat{L}^+ R. \quad (25)$$

In the following sections, the mistuning identification technique will be applied to the blisk presented in Section 2.2. First, the experimental investigations and the identification of measured data will be detailed. Then the results of the mistuning identification will be presented and discussed.

4. EXPERIMENTAL INVESTIGATIONS

4.1. Measurements

Experimental set-up

The experimental set-up is depicted in Figure 4. The structure of interest is the blisk described in Figures 1 and 2. As mentioned earlier, mistuning in bladed disks refers to small

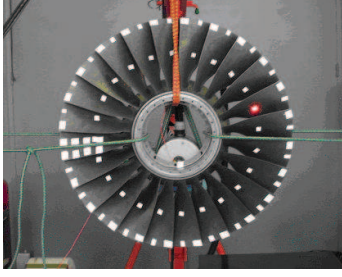


FIGURE 5: Excitation and force measurement.

perturbations of the structure's characteristics. As a consequence, we tried to avoid any external sources of perturbation in the experimental procedure. First, we chose a non-contacting measurement tool, which is a laser vibrometer. Then, we preferred a free boundary condition of the structure (with "soft" links compared to the structure natural frequencies) to a clamped one which may perturb the dynamics of the structure with an additional stiffness not taken into account in the model. It is held using soft links (rubber tighteners) which represent free boundary conditions. Also note that using velocimetry techniques eliminates the eventual measurement errors due to rigid body motions.

The blisk is excited using an electromagnetic shaker at one point located inside the rim of the blisk; a force transducer is then used to measure the input force (see Figure 5). We ensured that the additional mass (sensor) did not perturb the structure. In effect, we performed tests to study the influence of an additional (small) mass located near the excitation point on the dynamical response. The conclusion was that the perturbation (a frequency shift smaller than 0.1%) is far smaller than the phenomenon of interest here. Also, as the blisk is, in essence, a very weakly damped structure, this disk excitation provides sufficient level to excite the blades modes.

This experimental set-up described here is quite simple and this may contrast with other works that use more sophisticated procedure. We can, for example, mention the works of Feiner and Griffin [24] or Judge et al. [25] who proposed measurements on a nonfree structure with some travelling excitations. These methods allow to measure each modes with different nodal diameters separately whereas the present strategy allows the measurements of all modes simultaneously. Both methods have some advantages and drawbacks, the method with travelling excitations can limit the measurements errors but the experimental set-up is more important; the single-point excitation method is more adapted to industrial applications due to its simplicity.

Measurement procedure

The method model updating for mistuning identification proposed in this paper is based on the experimental knowledge of a system of modes, that is, a family of bladed disk modes for all nodal diameters in which the deformed shape of the blades are identical. The single-point excitation de-

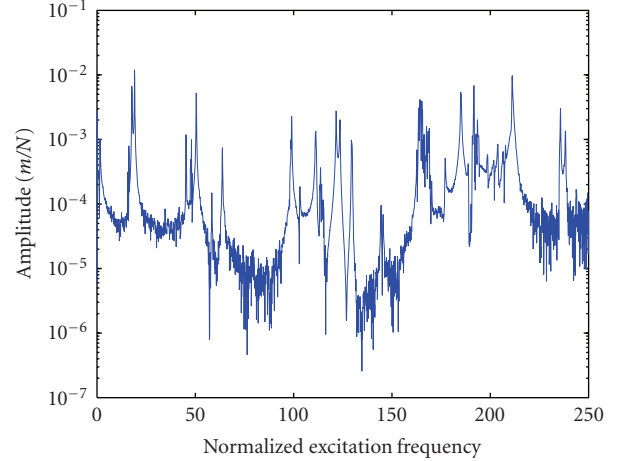


FIGURE 6: Wide frequency band measurement on a blade.

scribed in the previous paragraph allows the observation of all nodal diameter modes simultaneously in the frequency bandwidth of interest. The first step of the measurement procedure is to do a measurement on a large frequency range. In Figure 6, a global frequency response function (FRF) on a blade is represented and we can distinguish several groups of peaks each of which corresponding to a family of modes. Then, identifying the associated deformed shape, we can isolate a family of modes to work with. Next, a more precise measurement was done with a small frequency step,

$$\frac{\Delta f}{f} \approx 5 \cdot 10^{-5}. \quad (26)$$

One point on each blade (top-leading edge) was measured.

4.2. Modal identification

The proposed mistuning identification method uses measured modes and eigenfrequencies to update the reduced-order model. As a consequence, a modal identification of the experimental data is required. For a given frequency range, the identification was done on all measured FRFs simultaneously. The general expression of a transfer function from a point i to a point l is

$$h_{il}(\omega) = \sum_{k=1}^n \frac{x_{ik}x_{lk}}{\omega_k^2 - \omega^2 + 2j\omega\zeta_k}. \quad (27)$$

The first step is to identify the poles of the functions, then an estimation of the residues $x_{ik}x_{lk}$ is performed on the whole frequency band in order to fit all of the FRFs; a nonlinear optimization can also be performed on the poles to refine the identification. An example of identification for the first bending mode family is shown in Figure 7 where both measured and identified FRF (on a point of a blade) are superimposed together with the identified poles (in vertical dashed lines). The first remark is that for this first bending mode family the modal density is rather important. In effect,

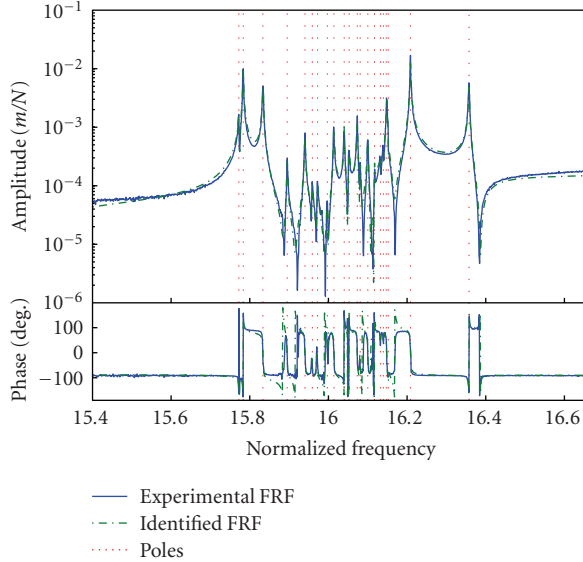


FIGURE 7: Modal identification.

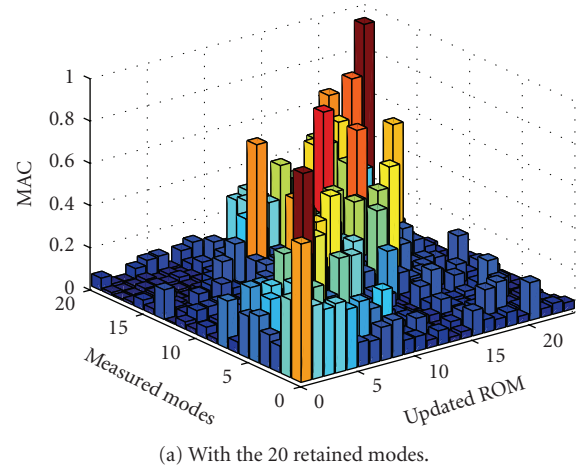
the chosen type of excitation (fixed, single-point excitation) leads to a response which includes all nodal diameter modes. Concerning the modal identification, we can see, in this example, that more poles were identified than the real number of modes in the frequency range. In effect, there are theoretically at the maximum 24 modes (corresponding to each possible nodal diameter) in the frequency range. The additional identified poles are necessary to properly fit the experimental curves. When the mistuning identification will be performed, a choice among this modes will be necessary; this will be detailed further.

5. IDENTIFICATION OF MISTUNING AND MODEL UPDATING

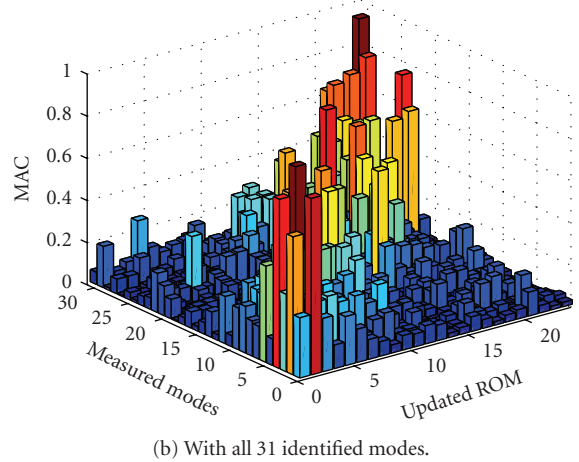
In this section, we applied the mistuning identification technique described in Section 3 to the bladed disk. We first focus on the blade's first bending mode family to update the model and find the associate mistuning parameter.

5.1. Identification results and correlation of modal responses

As mentioned earlier, the identification of modal data from the measured FRFs provides more poles than necessary, some of them have no physical signification. For the first bending mode, the modal identification provides 31 "modes" whereas there are theoretically 24 modes. Then we have to find the best set of modes to be retained. To find this optimal set of measured modes, we applied an iterative procedure. Starting from an initial (arbitrary) set of 20 measured modes and performing the mistuning identification, we find a first set of mistuning parameter (illustrated by symbol x in Figure 9). The average value of the mistuning is -19.70% and the standard deviation is 1.243% . The mean mistuning is quite important. In effect, the structure used for the experiments was



(a) With the 20 retained modes.



(b) With all 31 identified modes.

FIGURE 8: Modal correlation: 1st iteration.

an unfinished blisk (the blade geometry was not nominal due to an incomplete manufacturing process), which explains that the (tuned) FE model does not properly represent the real structure. However, the standard deviation is quite typical of bladed disks.

Then we compare the modal response of the updated model to the identified measured modes using a *modal assurance criterion* (MAC) matrix:

$$\text{MAC}(\mathbf{u}, \mathbf{v}) = \left(\frac{\mathbf{u}^T \cdot \mathbf{v}}{\|\mathbf{u}\| \|\mathbf{v}\|} \right)^2. \quad (28)$$

In Figure 8, we compare the modal correlation of the 24 modes given by the updated model to the 20 measured modes used for the identification (Figure 8(a)) and to the whole set of measured modes (Figure 8(b)).

It clearly appears that some of the measured modes that we have not initially retained for the identification (see Figure 8(b)) have a better correlation than some we have retained.

These observations, based on the modal assurance criteria, were then used as an empirical criterion for the optimal choice of measured data. The set of retained modes

TABLE 1: Statistic values of identified mistuning at each iteration.

Iteration	E , mean mist.	σ , standard dev.
1	19.70%	1.243%
2	19.57%	1.299%
3	19.59%	1.278%

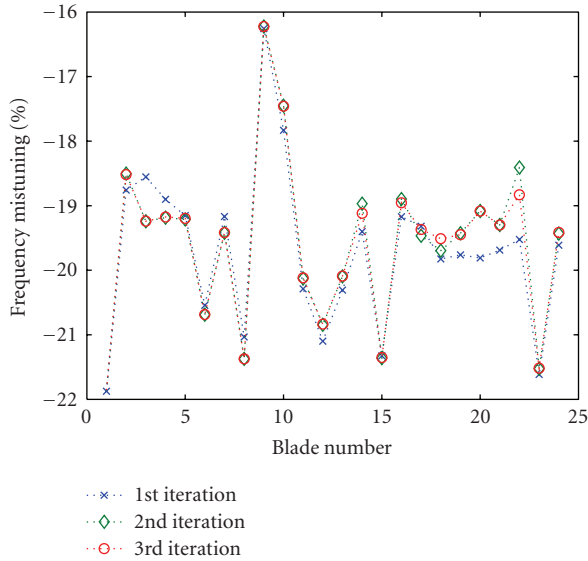


FIGURE 9: Mistuning parameters (% frequency).

is then changed, including the initially nonretained modes that present a better correlation and removing initially retained modes that have a poor correlation. A new identification/updating procedure is then performed. This iterative procedure leads to the elimination of some of the errors of measurement or of identification of modal data. In Figure 9, the mistuning parameters for each of the three iterations are represented and Table 1 gathers the statistical data of the identified mistuning; the global distribution of the mistuning among the blades is quite similar. However, if the mistuning distribution changes significantly from iteration 1 to iteration 2, the changes are minor in iteration 3 (see Figure 9). Then the iterative procedure appears to have converged.

The final modal correlation is shown in Figure 10 together with a plot (Figure 11) of the error in natural frequencies (normalized values and relative error) of updated reduced-order model and the measured ones. The results of these final iteration are acceptable. The maximum relative error in natural frequency does not exceed 1% which indicates that global frequency dispersion is well represented by the identification method. The modal correlation (Figure 10) shows some good correlations for some modes; however, some disparities appear particularly in high modal density regions. One explanation of these differences could be, as mentioned earlier, the quite important value of the average mistuning. This indicates that the FE model does not properly represent the virtual tuned model of the real blisk. This

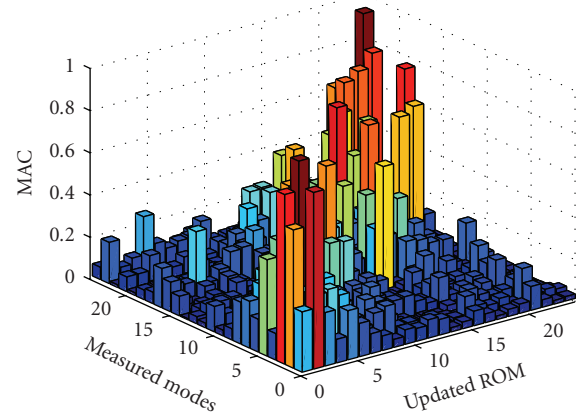


FIGURE 10: Modal correlation: final iteration.

can significantly affect the efficiency identification method and in particular the expansion and eigendata assignment steps since the measured data are projected on an achievable mistuned model which is derived from the tuned FE model. This issue is referred, in the literature, as a cyclic modelling error and maybe the use of techniques to overcome this error would increase the performance of the present method. The CMS-based method of Judge et al. was recently improved by including a cyclic correction procedure in [26]; on the other hand, the completely experimental method of Feiner and Griffin [27] also allows to overcome this problem.

5.2. Correlation of forced responses

In this final section, we present the correlation of the forced responses. We compare the measured FRFs to the forced response with the one point excitation computed with the ROM updated with the mistuning parameters previously identified. An example of correlation is shown in Figure 12. We can see that most of the peaks are correctly represented and located by the updated model and that the frequency deviation between the two curves is small in most cases. One can notice some differences in term of level between the experiment and the updated ROM. Several facts can explain these differences. First, the selection strategy for the identified modes described in Section 5.1 presents some difficulties and potential inaccuracy in this step can explain part of the observed discrepancies. However, the main reason may be an incorrect modelling of the damping in the ROM. In effect, since only the frequency mistuning has been identified, an arbitrary damping factor was introduced in the forced response simulations. It appears, from the identified/measured FRF, that the modal damping can vary significantly among the modes of a given family (about 40% from the mean value in worst cases); this, and the fact that this structure is very weakly damped, can explain some of the level differences in Figure 12. In contrast with these results, some authors (see, e.g., [13]) have presented test cases on dedicated test structures with controlled mistuning and some updating results with better correlation. Also, both the facts that

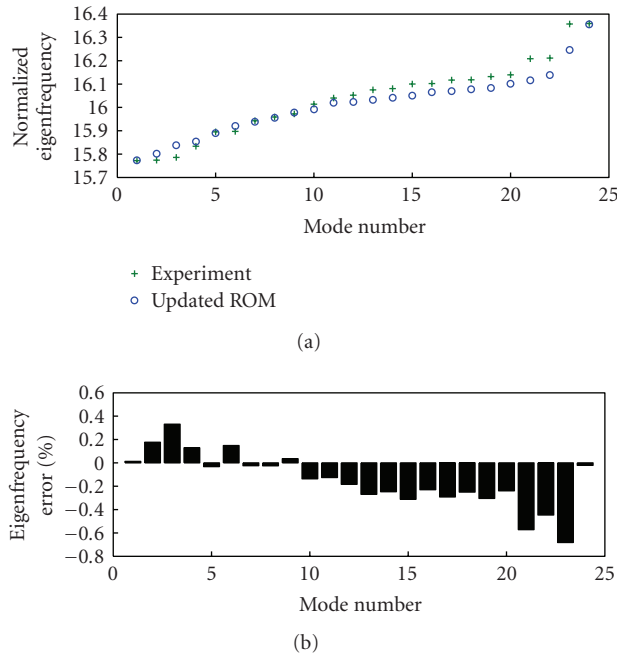


FIGURE 11: Error in natural frequencies.

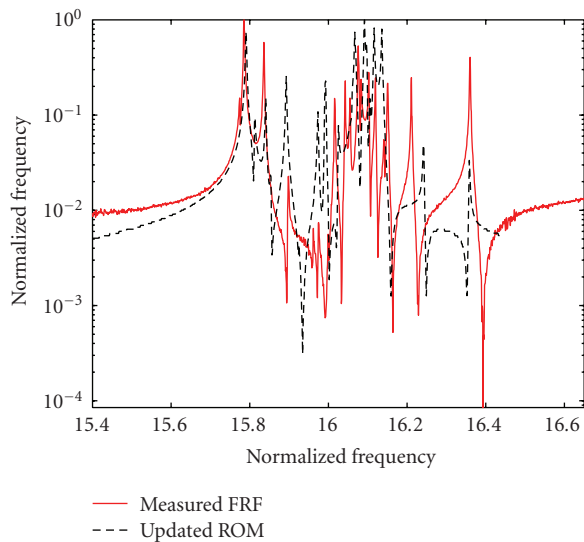


FIGURE 12: Forced response correlation.

the structure of interest in this paper appears more complex and that the FE model exhibits significant differences with the real structures can explain the inferior correlation presented here. However, regarding these results, the approximation made on the damping mistuning appears acceptable from an industrial point of view since the global dynamics of the mistuned bladed disk is quite well estimated. In effect, both the frequency dispersion and the amplification of the vibration level in blade due to mistuning are identified at least from a statistical point of view. This allows some statistical studies to be conducted using these identified information.

6. CONCLUSIONS

The results of an experimental investigation to identify the mistuning properties of a realistic industrial blisk (integrally bladed disk) was presented. The method of mistuning identification consists in updating a reduced-order model built using a component mode synthesis method with measurements of a system of modes of the structure as input. The experimental protocol is well adapted to industrial applications since it involves usual testing materials and since all modes of a given family can be measured simultaneously. One feature of the updating procedure presented and used in this paper is the regularization and eigenvalue assignment techniques which ensure a better representativeness of the measured data and increase the robustness of the method to measurement error.

The results of identification are acceptable regarding the modal correlation as well as the forced response correlation.

ACKNOWLEDGMENTS

Thanks go to Snecma for its technical and financial support. This work takes place in the framework of the MAIA mechanical research and technology program sponsored by CNRS, ONERA, and SAFRAN Group.

REFERENCES

- [1] A. V. Srinivasan, "Flutter and resonant vibration characteristics of engine blades," *Journal of Engineering for Gas Turbines and Power*, vol. 119, no. 4, pp. 742–775, 1997.
- [2] S.-T. Wei and C. Pierre, "Localization phenomena in mistuned assemblies with cyclic symmetry—part I: free vibrations," *Journal of Vibration, Acoustics, Stress, and Reliability in Design*, vol. 110, no. 4, pp. 429–438, 1988.
- [3] S.-T. Wei and C. Pierre, "Localization phenomena in mistuned assemblies with cyclic symmetry—part II: forced vibrations," *Journal of Vibration, Acoustics, Stress, and Reliability in Design*, vol. 110, no. 4, pp. 439–449, 1988.
- [4] M. P. Castanier, G. Óttarsson, and C. Pierre, "A reduced order modeling technique for mistuned bladed disks," *Journal of Vibration and Acoustics*, vol. 119, no. 3, pp. 439–447, 1997.
- [5] M.-T. Yang and J. H. Griffin, "A reduced-order model of mistuning using a subset of nominal system modes," *Journal of Engineering for Gas Turbines and Power*, vol. 123, no. 4, pp. 893–900, 2001.
- [6] E. Seinturier, C. Dupont, M. Berthillier, and M. Dumas, "A new method to predict flutter in presence of structural mistuning," in *Proceedings of the 9th International Symposium on Unsteady Aerodynamics, Aeroacoustics and Aeroelasticity of Turbomachines (ISUAAAT '00)*, Lyon, France, September 2000.
- [7] R. Bladh, M. P. Castanier, and C. Pierre, "Component-mode-based reduced order modeling techniques for mistuned bladed disks—part 1: theoretical models," *Journal of Engineering for Gas Turbines and Power*, vol. 123, no. 1, pp. 89–99, 2001.
- [8] D.-M. Tran, "Component mode synthesis methods using interface modes. Application to structures with cyclic symmetry," *Computers & Structures*, vol. 79, no. 2, pp. 209–222, 2001.
- [9] J. H. Griffin and T. M. Hoosac, "Model development and statistical investigation of turbine blade mistuning," *Journal of Vibration, Acoustics, Stress, and Reliability in Design*, vol. 106, no. 2, pp. 204–210, 1984.

- [10] A. Sinha, "Calculating the statistics of forced response of a mistuned bladed disk assembly," *AIAA Journal*, vol. 24, no. 11, pp. 1797–1801, 1986.
- [11] J. Judge, C. Pierre, and O. Mehmed, "Experimental investigation of mode localization and forced response amplitude magnification for a mistuned bladed disk," *Journal of Engineering for Gas Turbines and Power*, vol. 123, no. 4, pp. 940–950, 2001.
- [12] J. Judge, C. Pierre, and S. L. Ceccio, "Mistuning identification in bladed disks," in *Proceedings of the International Conference on Structural Dynamics Modeling*, Madeira Island, Portugal, 2002.
- [13] D. M. Feiner and J. H. Griffin, "Mistuning identification of bladed disks using a fundamental mistuning model—part I: theory," *Journal of Turbomachinery*, vol. 126, no. 1, pp. 150–158, 2004.
- [14] D. M. Feiner and J. H. Griffin, "Mistuning identification of bladed disks using a fundamental mistuning model—part II: application," *Journal of Turbomachinery*, vol. 126, no. 1, pp. 159–165, 2004.
- [15] F. Pichot, F. Thouverez, L. Jézéquel, and E. Seinturier, "Mistuning parameters identification of a bladed disk," *Key Engineering Materials*, vol. 204, no. 2, pp. 123–132, 2001.
- [16] T. W. Lim and T. A. L. Kashangaki, "Structural damage detection of space truss structures using best achievable eigenvectors," *AIAA Journal*, vol. 32, no. 5, pp. 1049–1057, 1994.
- [17] T. W. Lim, "Structural damage detection using constrained eigenstructure assignment," *Journal of Guidance, Control, and Dynamics*, vol. 18, no. 3, pp. 411–418, 1995.
- [18] F. Pichot, D. Laxalde, J.-J. Sinou, F. Thouverez, and J.-P. Lombard, "Mistuning identification for industrial blisks based on the best achievable eigenvector," *Computers & Structures*, vol. 84, no. 29–30, pp. 2033–2049, 2006.
- [19] R. Bladh, M. P. Castanier, and C. Pierre, "Component-mode-based reduced order modeling techniques for mistuned bladed disks—part 2: application," *Journal of Engineering for Gas Turbines and Power*, vol. 123, no. 1, pp. 100–108, 2001.
- [20] W. A. Benfield and R. F. Hruda, "Vibration analysis of structures by component mode substitution," *AIAA Journal*, vol. 9, no. 7, pp. 1255–1261, 1971.
- [21] R. R. Craig and M. C. C. Bampton, "Coupling of substructures for dynamical analysis," *AIAA Journal*, vol. 6, no. 7, pp. 1313–1319, 1968.
- [22] M. P. Mignolet, A. J. Rivas-Guerra, and J. P. Delor, "Identification of mistuning characteristics of bladed disks from free response data—part 1," *Journal of Engineering for Gas Turbines and Power*, vol. 123, no. 2, pp. 395–403, 2001.
- [23] F. Pichot, *Identification du désaccordage des disques aubages monoblocs*, Ph.D. thesis, École Centrale de Lyon, Lyon, France, 2002.
- [24] D. M. Feiner, J. H. Griffin, K. W. Jones, J. A. Kenyon, O. Mehmed, and A. P. Kurkov, "System identification of mistuned bladed disks from traveling wave response measurements," in *Proceedings of the ASME Design Engineering Technical Conferences (DETC '03)*, vol. 5 B, pp. 1231–1240, Chicago, Ill, USA, September 2003.
- [25] J. A. Judge, S. L. Ceccio, and C. Pierre, "Traveling-wave excitation and optical measurement techniques for non-contacting investigation of bladed disk dynamics," *The Shock and Vibration Digest*, vol. 35, no. 3, pp. 183–190, 2003.
- [26] S. H. Lim, C. Pierre, and M. P. Castanier, "Mistuning identification and reduced-order model updating for bladed disks based on a component mode mistuning technique," in *Proceedings of the 9th National Turbine Engine High Cycle Fatigue Conference*, Pinehurst, NC, USA, March 2004.
- [27] D. M. Feiner and J. H. Griffin, "A completely experimental method of mistuning identification in integrally bladed rotors," in *Proceedings of the 8th National Turbine Engine High Cycle Fatigue Conference*, Monterey, Calif, USA, April 2003.